HIGH-ORDER SPARSE RADON TRANSFORM FOR DEBLENDING OF SIMULTANEOUS SOURCE SEISMIC DATA

MIN WANG and YARU XUE

China University of Petroleum, State Key Laboratory of Petroleum Resources and Prospecting, Beijing 102249, P.R. China. christinewm@163.com

(Received July 27, 2017; revised version accepted January 15, 2018)

ABSTRACT

Wang, M. and Xue, Y., 2018. High-order sparse Radon transform for deblending of simultaneous source seismic data. *Journal of Seismic Exploration*, 27: 167-181.

This paper proposes an iterative high-order Radon transform based on matching pursuit (MP) algorithm to separate the blended seismic data. During each iteration, the matched subspace is picked by energy distribution in the high-order Radon domain. In thus small subspace, the high-order Radon transform is realized quickly to estimate the effective signals. The blending noise is then estimated by the estimate-deblended data with prior acquisition code and subtracted from the pseudo-deblended data. Thus an iteration is finished. The MP method shows more sparse than the iterative reweight least square method (IRLS). We compared the denoising effectiveness between these two methods. Synthetic and field data experiments prove that the matching pursuit algorithm has higher SNR and better denoising effectiveness than IRLS method.

KEY WORDS: high-order Radon transform, matching pursuit algorithm, sparse constraint; simultaneous source acquisition.

INTRODUCTION

In conventional seismic data acquisition, the time intervals between successive shots are enough large in order to avoid the overlap from adjacent sources. However, the large time intervals lead to significant increase of acquisition cost and decrease of acquisition efficiency. To cut down the cost of seismic surveys and improve the collection efficiency, it is beneficial to reduce the number of shots in the process of acquisition. Nevertheless, it will

0963-0651/18/$5.00

result in spatial aliasing due to the source sampling deficiency and then damage the quality of data processing. To overcome this issue, the concept of simultaneous source acquisition (Moerig et al., 2013) has been proposed and applied in seismic exploration (Aaron et al., 2009), particularly in marine seismic exploration (Gan et al., 2015b).

Simultaneous source acquisition fires more than one source with a small time dither and allows temporal overlap between source records. In the past several years, it has attracted much industry attention because of its lower acquisition cost and better seismic data (Zhang et al., 2013; Abma, 2014). There are two main methods to process the simultaneous source seismic data. The first one is direct imaging and waveform inversion (Xue et al., 2016b), which can be used to eliminate the noise caused by interference in some constraint (Gan et al., 2016d; Ebrahimi et al., 2017). The other is a first-separate and second-process strategy (Chen et al., 2013), which is known as "deblending" (Panagiotis et al., 2012). Recently, the possibility of imaging and inversion directly on the blended seismic data is paid an emerging attention to investigate and many researchers have got some encourageing results. Although there are some inspiring results has been achieved by direct imaging method, the currently preferred approach is also to focus on separating blended data into single source. In this paper, we only study on the deblending of simultaneous source seismic data.

The blended noise is incoherent in the common receiver gather, so some filtering operators can be straightforward applied into these coherency-promoting domains to remove the blended noise, which like we do for eliminating the random noise in traditional seismic data (Yang et al., 2015b; Huang et al., 2016a; Li et al., 2016b; Chen et al., 2017). Researchers have proposed many different filtering methods to separate the blended seismic data. According to the slope difference between the simultaneous sources in the shot domain, Hampson et al. (2008) proposed a method to remove the interference by using a simple dip filter. Mahdad (2012) implemented an iterative $f-k$ filter to separate the blended seismic data in the common receiver domain. Huo et al. (2012) and Chen (2014) used the median filtering to attenuate the blending interference in the midpoint domain. Gan et al. (2016c) introduced a structural-oriented median filter to separate the simultaneous source in the flattened dimension. Chen and Fomel (2015) removed the blending noise by a two-step filtering method without impairing the useful signals.

Another way to remove the blending interference is inversion. In this way, the separation problem is treated as an estimation problem and solved by using iteratively inversion to estimate the desired unblended data. A regularization term is usually required (Qu et al., 2016; Zu et al., 2016c) to obtain a stable estimation model since the ill-posed nature of such estimation problems. Currently exist several different iterative methods based on the sparsity constraint (Xue et al., 2013; Gan et al., 2016b; Wu et al., 2016; Xue et al., 2017). Doulgeris et al. (2010) combined the natures of the filtering and inversion approaches to propose an iterative estimation and subtraction

method. Abma et al. (2010) adopted a sparse constraint in the *f-k* domain to eliminate the blending noise. Chen et al. (2014) introduced an iterative deblending approach based on shaping regularization in the seislet domain. Xue et al. (2017) proposed an amplitude-preserving iterative method based on high-order Radon transform to remove the incoherent noise in the common receiver gathers. Compared to the filtering methods, the separation results by inversion methods usually lead to be better.

So far, many separation methods are proposed. In these methods, the inversion of the traditional sparse domain can suppress some blending noises. The amplitude-preserving iterative algorithm based on a high-order Radon transform (Xue et al., 2017) has considered the AVO characters of the seismic data and then improved the deblending precision. Due to the more and more reported about success of deblending, we are temping to find a more sophisticated way to optimize the deblending performance. In this paper, we propose an iterative high-order sparse Radon transform based on matching pursuit algorithm to separate the blended seismic data. This method has higher SNR and better deblending effectiveness, which are proved by synthetic and field examples.

THEORY

Simultaneous source seismic data model

Usually, the seismic records of simultaneous source acquisition are obtained by two shooting vessels, which can be regarded as the blending of two independent sources. The second source shoots with a random dithering compared to the first source, but the seismic records from both sources are collected in a traditional shot point timing cycle. Therefore, the simultaneous source seismic data model can be formulated as follows:

$$D^{obs} = D_1 + TD_2 \quad , \tag{1}$$

Here, D_1 and D_2 respectively denote the seismic data to be collected from the first source and the second source; D^{obs} is the blended seismic record and T denotes the dithering operator. In the common receiver domain, the profile D_1 is coherent and the profile TD_2 is incoherent, so we can realize the separation by many denoising methods which are adopted to the random noise attenuation.

According to eq. (1) we can get a extended formula to estimate D_2 by introducing a adjoint dithering operator T^H:

$$T^H D^{obs} = T^H D_1 + D_2 \quad , \tag{2}$$

Combine eqs. (1) and (2), we get an augmented model estimation problem:

$$D = \Gamma d \quad , \tag{3}$$

where

$$D = \begin{bmatrix} D^{obs} \\ T^H D^{obs} \end{bmatrix}, \quad \Gamma = \begin{bmatrix} I & T \\ T^H & I \end{bmatrix}, \quad d = \begin{bmatrix} D_1 \\ D_2 \end{bmatrix}. \tag{4}$$

In practical seismic acquisition, the trace number of simultaneous source seismic records is less than the trace gather number of single shooting. Due to the ill-poseness of the above function, we can adopt the sparse transformation and iterative method to acquire the above optimal solution.

Sparse transformation: high-order Radon transform based on matching pursuit

In eq. (3), d as the inversion parameter is coherent and sparse in some domain, but the noise in blended data D is incoherent. In order to distinguish useful signal from noise, we can transfer the model parameters of the data d to some transform domains. A transform operator L is introduced to represent the unblended data by $d = Lm$.

There are many sparse transformation methods and one of the most commonly used is the Radon transform. The classical high resolution Radon transform does not consider the AVO characters and will lose the amplitude variation. To realize AVO-preserving high resolution Radon transform, more parameters are needed to describe the AVO. The better method to describe the amplitude is orthogonal polynomial transform (Johansen et al., 1995). Combining the Radon transform with the orthogonal polynomial transform, we can get a high-order Radon transform which contains the summation of amplitude, gradient, curvature, and other high-order polynomial information of event amplitude. The forward high-order hyperbolic Radon transform can be described by the following

$$d(t,x) = \sum_j \sum_v m_j(\tau = \sqrt{t^2 - x^2 / v_i}, v) p_j(x) \quad , \tag{5}$$

where $\{p_j(x), j = 0,1,...,N\}$ are a set of unit orthogonal polynomials from offset coordinate x with N+1 sample. N+1 is the number of the basis function $p_j(x)$, and each basis function $p_j(x)$ has the general form of a polynomial of degree j.

The second-order Radon transform can be formulated in matrix form as:

$$d = \begin{bmatrix} L_0 & L_1 & L_2 \end{bmatrix} \begin{bmatrix} m_0 \\ m_1 \\ m_2 \end{bmatrix} = Lm \quad , \tag{6}$$

where m_0 denotes the superposition of the amplitude and L_0 is the summation operator. m_1 is the amplitude gradient and L_1 denotes the gradient operator. m_2 is the amplitude curvature and L_2 is the curvature operator. The L_0, L_1, L_2 here refer to the zero-order characteristics, the gradient characteristics, and the curvature characteristics of the amplitude, respectively. We also have some other forms of composite Radon transform, such as the hybrid linear-hyperbolic Radon transform (Trad et al., 2001). The L_1 and L_2 in his paper are directed against linear and hyperbolic Radon transform on the path. These two different combinations are used to deal with amplitude characteristics and path characteristics, respectively.

Obviously, this formulation involves more unknown parameters and leads to increase the computational cost. The conventional method is to optimize the following objective function:

$$J = \left\| d - \Gamma L m \right\|_2^2 + \mu R(m) \quad , \tag{7}$$

where $R(m)$ is the regular function, which determine the distribution of model m. The non-quatratic regularization is introduced to suppress the ringing in the inversion results and iterative reweighted least square algorithm is achieved following (Sacchi et al., 1995):

$$m = \left[(\Gamma L)^T \Gamma L + \mu Q(m) \right]^{-1} (\Gamma L) d \quad , \tag{8}$$

where $Q(m)$ is the derivative of regular function $R(m)$. The larger the model, the smaller the weighted function $Q(m)$.

For the blended data, the energy of interfere noise is almost balanced with the coherent signals and results some noise models little smaller than the ones of signals in the Radon domain. To solve this problem, we use the matching pursuit to pick the inversion space carefully and decrease the computational cost. In this method, the main velocity parameters are chosen by energy distribution in the Radon domain. The bigger the parameter energy is, the earlier the parameter is selected. The algorithm can be modified from equation and follows:

$$m = \left[(\Gamma L)^T \Gamma L \right]_{th}^{-1} (\Gamma L) d \quad . \tag{9}$$

The subscript th means threshold which determines the subspace dimensions. In each iteration, the inversion subspace is only constituted by a small subset of parameters and the computation efficiency is improved.

In the high-order Radon domain, the energy distribution along different velocity at intercept τ is described as follows:

$$E(\tau, v) = \sum_{j=0}^{2} m_j^2(\tau, v). \tag{10}$$

According to the energy distribution, we can find the maximum energy $e_{\max}$, and then set the threshold as follows:

$$e = \sigma e_{\max} \quad , \tag{11}$$

where e is any element of the $E(\tau, v)$. The parameter σ is a weighting factor that usually set by experience. We can choose the velocity parameter model according to the threshold, and then use the velocity gather to estimate the useful signal. Through threshold selection, the data of high-order Radon domain becomes more sparse, thus the resolution of the Radon transform is improved. The parameter σ is closely related to the sparsity of data in Radon domain. The larger the value of the parameter σ, the greater the sparseness of the data. If the data sparsity is too high, the most part of the useful signal is lost. Conversely, if the sparsity is too low, the noise is mixed. Therefore, we need to select a suitable value of σ to optimize the algorithm.

ITERATIVE METHOD

The effective signal without noise can be obtained by using the high-order Radon transform based on the above matching pursuit. However, duo to the limitation of threshold selection, a small amount of the useful signal energy will be lost. Therefore, in order to improve the quality of deblending, iterative algorithm is introduced to optimize the deblended results. In this iterative algorithm, the original blended data is processed by a high-order Radon transform based on matching pursuit and the estimated unblended data is achieved. The noise is estimated by using the dithering code, and then the estimated unblended data and the estimated noise are subtracted from the blended data. The calculated result is input for next iteration. Finally, the noise is estimated by the superposition of each estimated unblended data, and removed from the original blended data to obtain the deblending data.

The stopping criterion of the iterative algorithm is the norm of the different between the original blended data and the estimated blended data. The iteration will stop when this value is less than the set threshold. Thus we can control the degree of data fitting by controlling the misfit to observation error.

All of the above algorithms can be implemented with the following pseudo code:

Inputs:

The blended data D^{obs}, dither operator T and error threshold δ.

Initialize:

$$\hat{D}_1 = D^{obs}, \quad \hat{D}_2 = T^H D^{obs}; \quad D_{1\_re} = 0, \quad D_{2\_re} = 0.$$

Iteration:

1. Compute the least squares solutions of high-order Radon transform

$\hat{m}_1$ and $\hat{m}_2$ of data $\hat{D}_1$, $\hat{D}_2$ using eq. (7).

2. Use the matching pursuit method to choose the main velocity parameters subspaces V_1 and V_2 in the high-order Radon domain, which is computed by eq. (8).

3. Estimate the D_{1_es}, D_{2_es} from $\hat{D}_1$, $\hat{D}_2$ by inverse and forward high-order Radon transform in the above subspace.

4. Update the estimated unblended data by

$D_{1\_re} = D_{1\_re} + D_{1\_es}, D_{2\_re} = D_{2\_re} + D_{2\_es}$, and update the blended data by

$$\hat{D}_1 = \hat{D}_1 - D_{1\_es} - TD_{2\_es}, \hat{D}_2 = \hat{D}_2 - D_{2\_es} - T^H D_{1\_es}.$$

5. Get the denoised data by

$$D_{1\_db} = D^{obs} - TD_{2\_re}, D_{2\_db} = T^H D^{obs} - T^H D_{1\_re}.$$

6. Compute the blended data by $\hat{D}^{obs} = D_{1\_db} + TD_{2\_db}$.

7. If $\left\| D^{obs} - \hat{D}^{obs} \right\| < \delta$ end

Else Return to 1.

The matching pursuit method is applied to high-order Radon transform, which improves the sparsity of data and then improves the resolution of

Radon transform. The iterative algorithm will optimize the deblending result and improve the deblending quality greatly.

EXAMPLES

Synthetic data example

To test the feasibility and effectiveness of the proposed deblending method, we designed a convolution model to prove it. First, the seismic data is synthesized by convolving predefined reflectivity with the Ricker wavelet, which has six events and the amplitude of the event varies with the offset. We assumed that the simultaneous-source data is blended using two independent sources that correspond to two shooting sources in the conventional acquisition. In the common receiver domain, one source of the original unblended data is shown in Fig. 1(a). The blending noise is created by

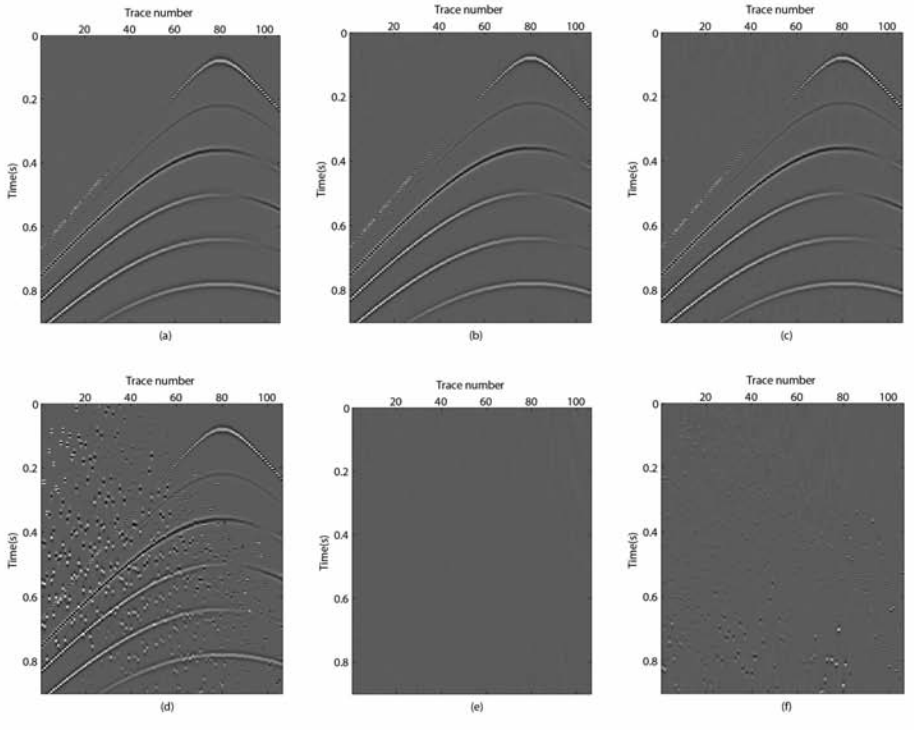

Fig. 1. Deblending comparison for the synthetic data in Common Receiver Gathers (CRG). (a) The original CRG data. (b) The deblended data using the matching pursuit iterative method. (c) The deblended data using the IRLS method. (d) The blended data. (e) Error displays for (b) (which is amplified 10 times). (f) Error displays for (c) (which is amplified 10 times).

applying the dithering code varying within 450 ms to the unblended data of the second source. The blended data is shown in Fig. 1(d). In this figure, we can see that the useful signals are seriously contaminated by the blending noise. Fig. 1(b) shows the deblended result after processing by the matching pursuit iterative method. Fig. 1(c) shows the deblended result that is obtained using the IRLS method, which has been used as shaping regularization in another paper (Xue et al., 2017). From Figs. 1(b) and 1(c), we can see all the useful hyperbolic events are recovered and any evident blending noise is not existed. It is hard to find the differences between the two deblended results, so we give the errors in Figs. 1(e) and 1(f), which show the error of Fig. 1(b) and the error of Fig. 1(c), respectively.

Comparing Figs. 1(e) and 1(f), we clearly find that a part of noise was not removed in Fig. 1(f). However, there is no significant noise left in Fig. 1(e). This is because the matching pursuit iterative method can only select the energy of coherent signals in the Radon domain, which can improve the sparsity of the data, and thus improve the resolution of the Radon transform. The coherent signals estimated by this method are free of noise and have higher accuracy. Thus, the noise estimated by the coherent signals is more accurate and the deblended effect is better.

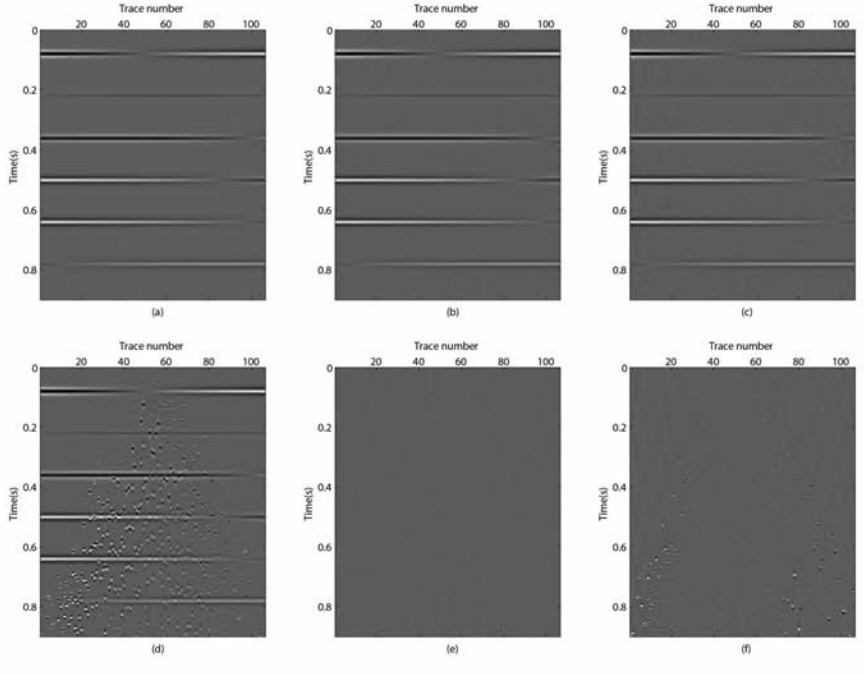

Fig. 2. Deblending comparison for the synthetic data in Common Offset Gathers (COG). (a) The original COG data. (b) The deblended data using the matching pursuit iterative method. (c) The deblended data using the IRLS method. (d) The blended data. (e) Error displays for (b)(which is amplified 10 times). (f) Error displays for (c)(which is amplified 10 times).

To comprehensively analyze the deblended results, we also observed the deblended results in the common offset domain. One independent source is shown in Fig. 2(a). Fig. 2(d) shows the blended data. The deblended result of the matching pursuit iterative method is shown in Fig. 2(b). We used the IRLS method to process the blended data, and the result is shown in Fig. 2(c). Figs. 2(e) and 2(f) show the error of Fig. 2(b) and the error of Fig. 2(c), respectively. It is obviously that both methods can remove the blended noise and not harm the main events from Fig. 2(b) and Fig. 2(c). But, there is visible residual noise can be seen in Fig. 2(f). The comparison shows that it is better to separate the blended data by the matching pursuit iterative method than the IRLS method.

In order to quantitatively analyze the problems, we plotted the SNRs of the common receiver gathers from the matching pursuit iterative method and the IRLS method. Fig. 3 shows the SNRs varies with the number of iterations. The solid line shows the SNR of the matching pursuit iterative method, which can be seen that the SNR increase gradually. The dashed line shows the SNR of the IRLS method, which does not change after several iteration. Comparing the SNRs of both methods, the matching pursuit iterative method can reach a higher SNR than the IRLS method.

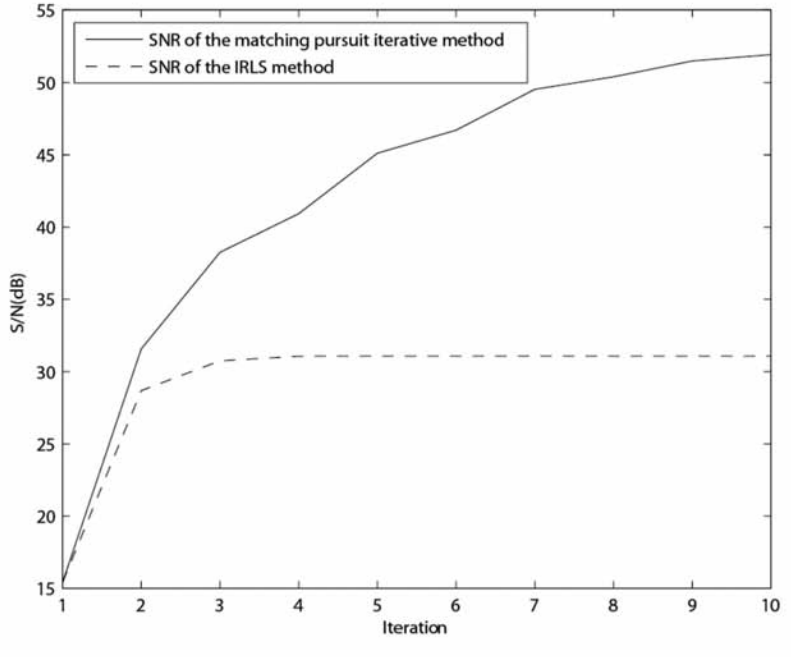

Fig. 3. Diagrams of SNR for the two different methods. The solid line corresponds to the matching pursuit iterative method. The dashed line corresponds to the IRLS method.

FIELD DATA EXAMPLE

In this part, we used a real marine data to test the effectiveness of the proposed algorithm. The data is from a real acquisition system, which has 220 shots and 320 receivers in total, the trace interval is 25 m, the sampling interval is 4 ms, and the sampling duration is 4 s. Fig. 4(a) shows the original common receiver gather data from one source. Fig. 4(d) shows the blended data which blends by 2 simultaneous shooting sources. There is a random time dither between the main source and another source. From Fig. 4(d), we can see that the useful signals are coherent in the common receive domain, but the interference is not coherent. The deblended results of the matching pursuit iterative method and the IRLS method are shown in Figs. 4(b) and 4(c), respectively. Comparing Fig. 4(b) and Fig. 4(c), we can see subtle differences between them. In order to analyze the effect of separation more intuitively, we compare the errors of the two deblending methods, which are shown in Figs. 4(e) and 4(f), respectively. It is obviously that the deblended result of the matching pursuit iterative method is better than the IRLS method.

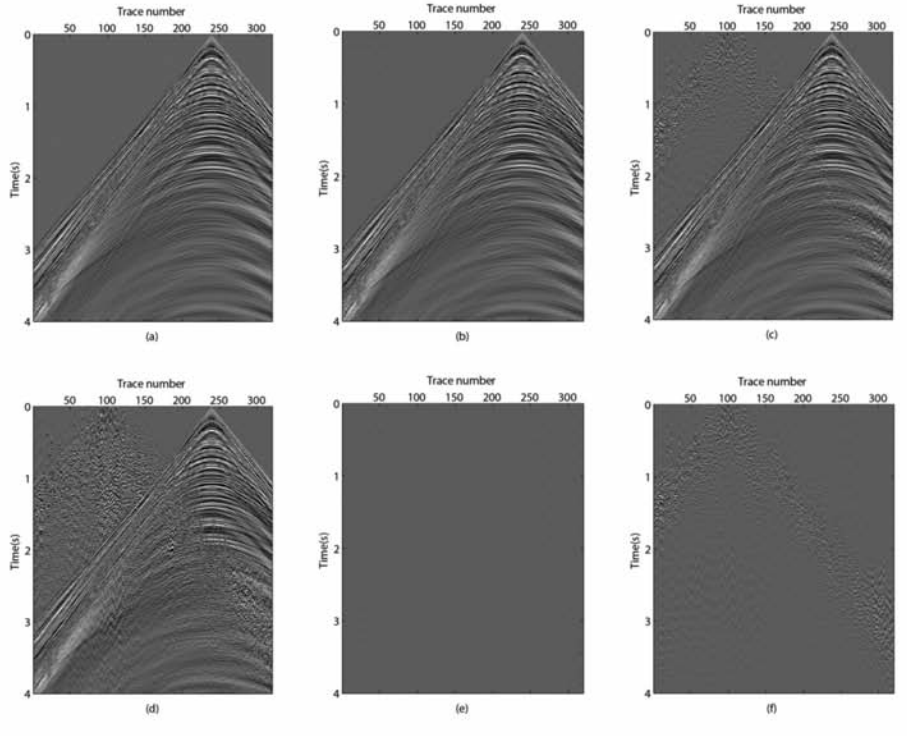

Fig. 4. Field data deblending comparison in CRG. (a) The original CRG data. (b) The deblended data using the matching pursuit iterative method. (c) The deblended data using the IRLS method. (d) The blended data. (e) Error displays for (b). (f) Error displays for (c).

We also analyze the deblended results in the common offset domain. Fig. 5(a) shows the original common offset gather data. The blended data is shown in Fig. 5(d), which can be seen that there is a lot of interference. Figs. 5(b) and 5(c) are shown the deblended results of the matching pursuit iterative method and the IRLS method, respectively. The errors of Figs. 5(b) and 5(c) are shown in Figs. 5(e) and 5(f), respectively. The comparison shows that our method can obtain a better deblended result than the IRLS method.

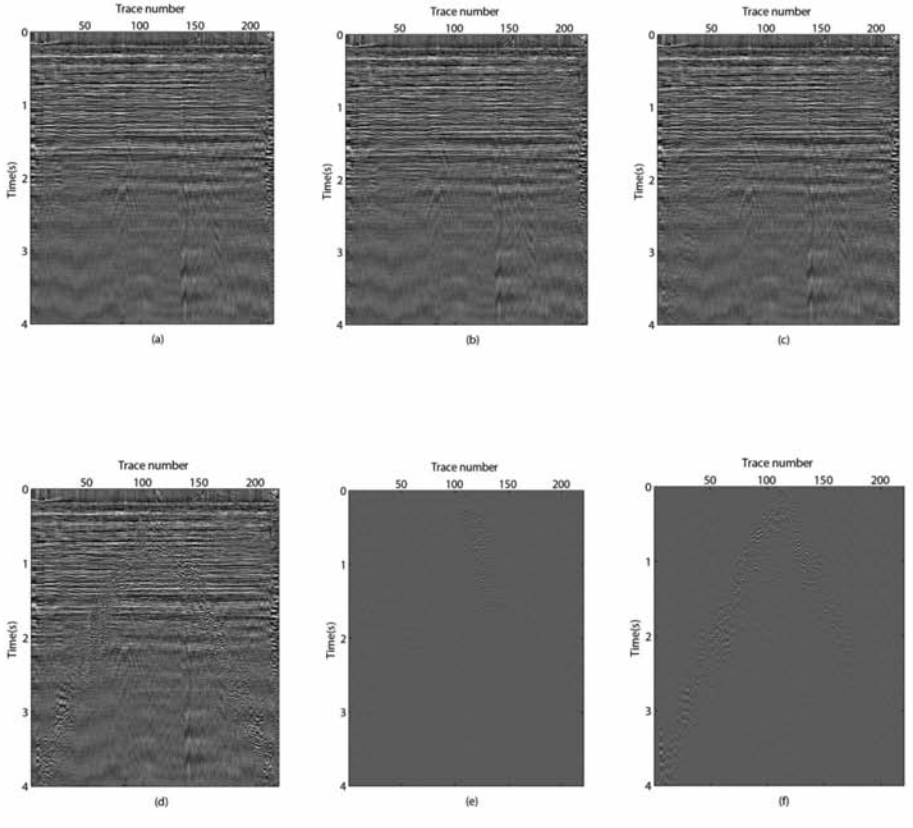

Fig. 5. Field data deblending comparison in COG. (a) The original COG data. (b) The deblended data using the matching pursuit iterative method. (c) The deblended data using the IRLS method. (d) The blended data. (e) Error displays for (b). (f) Error displays for (c).

Fig. 6 shows the SNRs of the deblended results. The solid line, corresponding to the matching pursuit iterative method, is rising gradually. The dashed line, corresponding to the IRLS method, remains the same after several iterations. From the Fig. 6, we can see that the matching pursuit iterative method can achieve a higher SNR compared with the IRLS method for the same dithering range.

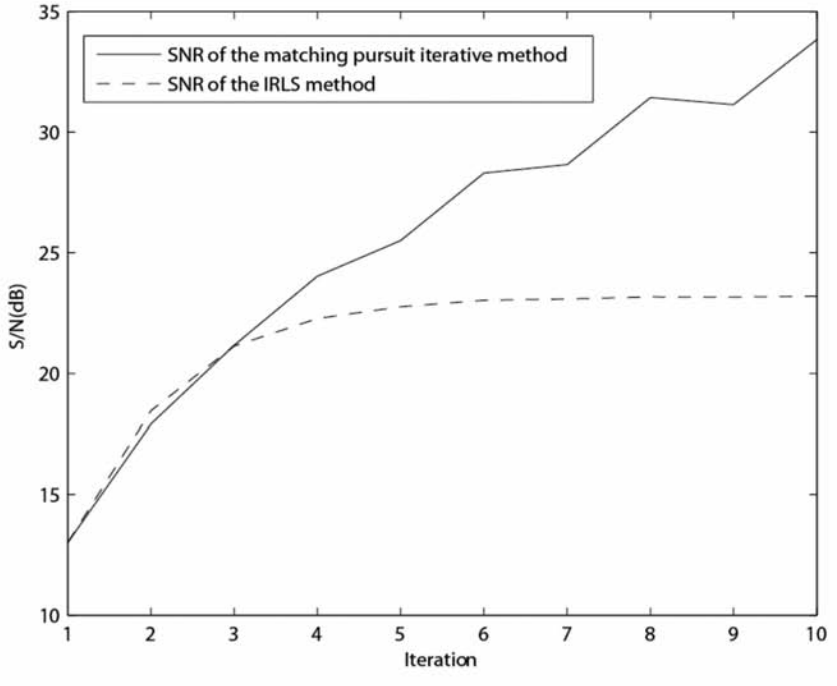

Fig. 6. Diagrams of SNR for the two different methods. The solid line corresponds to the matching pursuit iterative method. The dashed line corresponds to the IRLS method.

CONCLUSIONS

High-order Radon transform is a combination of conventional Radon transform and orthogonal polynomial transform, and it has very strong amplitude preservation. In this paper, we introduce the matching pursuit method into the high-order Radon transform, which increases the sparsity of the data in the high-order Radon domain, improves the resolution of the high-order Radon transform, and accelerates the speed of the high-order Radon transform. Due to the limitations of threshold selection, although the

coherent signals obtained after one processing do not contain any noise, a small amount of energy is lost. So we design an iterative algorithm to estimate the useful signal accurately, then to obtain accurate noise estimation and realize the separation of the coherent signal and incoherent noise. The method only selects the main energy of the useful signal in each iteration, so it can estimate the noise accurately and remove the noise from the blended data effectively. Experiments on synthetic data and field data show that the proposed method can obtain more accurate deblended result.

REFERENCES

Aaron, P., van Borselen, R. and Fromyr, E., 2009. Simultaneous sources: a controlled experiment on different source configurations. Expanded. Abstr., 79th Ann. Internat. SEG Mtg., Houston: 1177-1181.

Abma, R., 2014. Shot scheduling in simultaneous shooting. Expanded Abstr., 84th Ann. Internat. SEG Mtg., Denver: 94-98.

Abma, R.L., Manning, T., Tanis, M., Yu, J. and Foster, M., 2010. High-quality separation of simultaneous sources by sparse inversion. Extended Abstr., 72nd EAGE Conf., Barcelona: B003.

Chen, W., Yuan, J., Chen, Y. and Gan, S., 2017. Preparing the initial model for iterative deblending by median filtering. J. Seismic Explor., 26: 25-47.

Chen, Y., 2014. Deblending using a space-varying median filter. Explor. Geophys., 46: 51-83.

Chen, Y. and Fomel, S., 2015. Random noise attenuation using local signal-and-noise orthogonalization. Geophysics, 80: WD1-WD9.

Chen, Y., Fomel, S. and Hu, J., 2013. Iterative deblending of simultaneous-source seismic data using shaping regularization. Expanded Abstr., 83rd Ann. Internat. SEG Mtg., Houston: 119-125.

Chen, Y., Fomel, S. and Hu, J., 2014. Iterative deblending of simultaneous-source seismic data using seislet-domain shaping regularization. Geophysics, 79: V179-V189.

Doulgeris, P., Mahdad, A. and Blacquière, G., 2010. Separation of blended data by iterative estimation and subtraction of interference noise. Geophysics, 76: 44-53.

Ebrahimi, S., Kahoo, A.R., Chen, Y. and Porsani, M.J., 2017. A high-resolution weighted AB semblance foe dealing with amplitude-variation-with-offset phenomenon. Geophysics, 82(2): V85-V93.

Gan, S., Wang, S., Chen, Y. and Chen, X., 2015b. Deblending of distance separated simultaneous-source data using seislet frames in the shot domain. Expanded Abstr., 85th Ann. Internat. SEG Mtg., New Orleans: 65-70.

Gan, S., Wang, S., Chen, Y. and Chen, X., 2016b. Simultaneous-source separation using iterative seislet-frame thresholding. IEEE Geosci. Remote Sens. Lett., 13: 197-201.

Gan, S., Wang, S., Chen, Y., Chen, X. and Xiang, K., 2016c. Separation of simultaneous sources using a structural-oriented median filter in the flattened dimension. Comput. Geosci., 86: 46-54.

Gan, S., Wang, S., Chen, Y., Qu, S. and Zu, S., 2016d. Velocity analysis of simultaneous-source data using high-resolution semblance-coping with the strong noise. Geophys. J. Internat., 204: 768-779.

Hampson, G., Stefani, J. and Herkenhoff, F., 2008. Acquisition using simultaneous sources. The Leading Edge, 27: 16.

Huang, W., Wang, R., Chen, Y., Li, H. and Gan, S., 2016a. Damped multichannel singular spectrum analysis for 3D random noise attenuation. Geophysics, 81: V261-V270.

Huo, S., Luo, Y. and Kelamis, P.G., 2012. Simultaneous sources separation via multidirectional vector-median filtering. Geophysics, 77: V123-V131.

Johansen, T.A., Bruland, L. and Lutro, J., 1995. Tracking the amplitude versus offset by using orthogonal polynomials. Geophys. Prosp., 245-261.

Li, H., Wang, R., Cao, S., Chen, Y., Tian, N. and Chen, X., 2016b. Weak signal detection using multiscale morphology in microseismic monitoring. J. Appl. Geophys., 133: 39-49.

Mahdad, A., 2012. Deblending of Seismic Data. Ph.D. thesis, Delft University of Technology.

Moerig, R., Barr, F.J. and Nyland, D.L., 2013. Simultaneous shooting using cascaded sweeps. Expanded Abstr., 83rd Ann. Internat. SEG Mtg., Houston: 74.

Panagiotis, D., Kenneth, B., Gary, H. and Gerrit, B., 2012. Convergence analysis of a coherency-constrained inversion for the separation of blended data. Geophys. Prospect., 60: 769-781.

Qu, S., Zhou, H., Liu, R., Chen, Y., Zu, S., Yu, S. and Yuan, Y., 2016. Deblending of simultaneous-source seismic data using fast iterative shrinkage-thresholding algorithm with firm-thresholding. Acta Geophys., 64: 1064-1092.

Sacchi, M.D. and Ulrych, T.J., 1995. High-resolution velocity gathers and offset space reconstruction . Geophysics, 60: 1169-1177.

Trad, D., Sacchi, M.D. and Ulrych, T.J., 2001. A hybrid linear-hyperbolic Radon transform. J. Seismic Explor., 9: 303-318.

Wu, J., Wang, R., Chen, Y., Zhang, Y., Gan, S. and Zhou, C., 2016. Multiples attenuation using shaping regularization with seislet domain sparsity constraint. J. Seismic Explor., 25: 1-9.

Xue, Y., Ma, J. and Chen, X., 2013. High-order high-resolution Radon transform for AVO-preservation multiples attenuation. J. Seismic Explor., 22: 93-104.

Xue, Y., Man, M., Zu, S., Chang, F. and Chen, Y., 2017. Amplitude-preserving iterative deblending of simultaneous source seismic data using high-order Radon transform. J. Appl. Geophys., 139: 79-90.

Xue, Z., Chen, Y., Fomel, S. and Sun, J., 2016b. Seismic imaging of incomplete data and simultaneous-source data using least-squares reverse time migration with shaping regularization. Geophysics, 81: S11-S20.

Yang, W., Wang, R., Wu, J., Chen, Y., Gan, S. and Zhong, W., 2015b. An efficient and efficient common reflection surface stacking approach using local similarity and plane-wave flattening. J. Appl. Geophys., 117: 67-72.

Zhang, Q., Abma, R. and Ahmed, I., 2013. A marine node simultaneous source acquisition trial at atlantis, gulf of mexico. Expanded Abstr., 83rd Ann. Internat. SEG Mtg., Houston: 99-103.

Zu, S., Zhou, H., Chen, Y., Pan, X., Gan, S. and Zhang, D., 2016c. Interpolating big gaps using inversion with slope constraint. IEEE Geosci. Remote Sens. Lett., 13: 1369-1373.